

# Lipids monitoring in *Scenedesmus obliquus* based on Terahertz Technology

**Yongni Shao**

University of Shanghai for Science and Technology

**Weimin Gu**

University of Shanghai for Science and Technology

**Yating Qiu**

University of Shanghai for Science and Technology

**Shengfeng Wang**

University of Shanghai for Science and Technology

**Yan Peng** (✉ [py@usst.edu.cn](mailto:py@usst.edu.cn))

University of Shanghai for Science and Technology <https://orcid.org/0000-0002-8273-5566>

**YiMing Zhu**

University of Shanghai for Science and Technology

**Songlin Zhuang**

University of Shanghai for Science and Technology

---

## Research

**Keywords:** Terahertz, Microalgae, Lipids

**Posted Date:** April 17th, 2020

**DOI:** <https://doi.org/10.21203/rs.3.rs-22335/v1>

**License:**   This work is licensed under a Creative Commons Attribution 4.0 International License.

[Read Full License](#)

---

**Version of Record:** A version of this preprint was published on September 16th, 2020. See the published version at <https://doi.org/10.1186/s13068-020-01801-0>.

# Abstract

## Background

Microalgae are considered as a source of low pollution and renewable fuel due to their ability to synthesize an abundance of lipids. Conventional methods for lipid quantification are time consuming and chemically contaminated. Spectroscopic method combined with mathematical model can be used for qualitative and quantitative analysis of material composition. Terahertz technology provides not only timely and nondestructive testing without chemical pollution, but also information about the functional group vibration mode and structure of the measured components. Therefore, terahertz is proposed for microalgae metabolism detection.

## Results

The aim of this study was to use Terahertz (THz) spectroscopy to observe lipid content in *Scenedesmus obliquus* (*S. obliquus*). We collected the THz spectra of *S. obliquus* which were cultivated under nitrogen stress and THz spectroscopy was used to analyze changes in substance components (lipids, proteins, carbohydrates and  $\beta$ -carotene). Partial least square was used to establish the prediction model of each stress time point. The correlation coefficient of the prediction results of the model was above 0.991, and the root mean square error was less than 0.020. It indicated that THz technology can be used to discriminate *S. obliquus* cells under different nitrogen stress culture times effectively. The correlation between the THz characteristic peak (9.3 THz) and the total lipid content determined by gravimetry reaches 0.96. The final results were compared with the commonly used spectroscopic methods for lipid observation (Raman spectroscopy).

## Conclusions

The prediction accuracy of model of THz bands is relatively high. It indicated that THz technology can be used to monitor the change of material composition in microalgae under nitrogen stress. THz is more accurate than Raman in total lipid monitoring. For the research of microalgal metabolites, compared with Raman technology, there is more research space for THz technology. THz technology can provide technical supporting for the engineering culture of oil-producing microalgae under environmental control in future.

## Background

Nowadays, global energy crisis continuously intensifies, which has raised interest in looking for low pollution and renewable energy resources. Among the many new energy sources, biodiesel has become the world's fastest growing and the most widely used clean renewable energy. As an important renewable resource, algae has the advantages of high photosynthetic efficiency, strong environmental adaptability

and short growth cycle [1]. In order to provide better strategies for process conditions, nutritional schemes, and metabolic engineering techniques, researchers have studied the microalgal metabolic processes [2]. For example, under nitrogen stress, changes in lipid accumulation in microalgae cells provide conditions for studying the mechanism of lipid accumulation [3–5].

When the biodiesel is produced by microalgae, the content of lipids and types of fatty acids in cells are the important considerations [6]. In this process, the screening of high quality microalgae and the monitoring of culture process are important for the efficient conversion of lipids. If the lipid content and distribution under nitrogen stress can be observed, a comprehensive understanding of lipid accumulation in microalgae cells can be obtained. However, the conventional methods for the quantitative analysis of microalgae lipids, gas chromatography-mass spectrometry (GC-MS) can accurately analyze lipid components, but the detection is time-consuming, and the sample preparation process is complicated, and cannot analyze the lipid metabolism process in cells. Nile red (NR) or BODIPY 505/515 can show lipid distribution in cells but the fluorescence intensity is affected by many factors, such as emission wavelength, dye concentration, cell density and staining time [7–9]. Therefore, it is necessary to find a fast and non-destructive method for detecting lipid content.

Spectroscopic method combined with mathematical model can be used for qualitative and quantitative analysis of material composition [10, 11], the technique provides not only timely and nondestructive testing without chemical pollution (such as extraction and esterification), but also information about the functional group vibration mode and structure of the measured components. For example, non-polar groups such as C=C, C-C, etc. have strong Raman activity [12]. Raman spectroscopy can reflect the differences in sample chemical composition and molecular structure at the molecular level, and achieve "fingerprint identification" of certain chemical bonds and functional groups in the molecule. The disadvantage of Raman spectroscopy is the strong Raman signal of pigments ( $\beta$ -carotene, Chlorophyll a, etc.), which overlaps with the Raman intensity of the lipid and interferes with measurement accuracy [13]. With the development of spectroscopy techniques, other spectroscopy techniques have also been tried to study microbial metabolism, such as Terahertz (THz) spectroscopy.

THz waves range from 0.1–20 THz, which is between the microwave and IR regions. THz has the advantages of fast analyzing speed, no chemical pollution, and no complex sample processing. It is suitable for large-scale sample testing [14]. The molecular structure of a compound is identified based on its characteristic absorption, so that the qualitative and quantitative analysis of the substance can be performed [15, 16]. In contrast to the conventional IR and Raman spectra, which mainly reflect intramolecular vibrations, the spectral information in the terahertz region is rich in collective modes such as intermolecular and backbone vibrations, which is more directly related to the molecular structure [17–19]. Therefore, THz signal can be a useful complement to the Raman and IR spectroscopy for monitoring microbial metabolism. In the past, researchers have used THz to do some research on microorganisms [20, 21], such as distinguishing *Escherichia coli*, *Bacillus subtilis* and *Bacillus species*. THz spectroscopy may become a new technique for detecting metabolites of microalgae cells, which is suitable for macroscopic detection in metabolic engineering [22–24]. However, due to the complexity of

vegetative cell components, there are no obvious characteristic peaks in the cell spectrum [20], and related reports lack the quantification of metabolites in cells [14]. Researchers prefer to conduct separate studies of cellular components outside the cell, such as fatty acids and their analogues distinction [25, 26], protein-structure recognition [15], starch quantification [16], forgetting the research of terahertz in the process of microalgae metabolism. Therefore, it is of great significance to use terahertz to study the metabolic process of microalgae lipids accumulation.

In this study, THz spectroscopy were used to observe the accumulation of lipids in *Scenedesmus obliquus* (*S. obliquus*). Gravimetric method, NR and GC-MS were used to validation the change of lipids under nitrogen stress. We collected the THz spectra of *S. obliquus* which were cultivated under nitrogen stress at different time from day 0 to day 10 with 2 days' collection interval, and identified the main components in the *S. obliquus* according to their THz characteristic peaks, including lipids, carbohydrates, carotenoids and proteins. Their variation rules of the content as a function of the grown days of *S. obliquus* were also analyzed. Principal component analysis (PCA) and partial least square(PLS) were used to distinguish and predict microalgae from different stress days. In addition, the correlation model between the total lipid content measured by THz spectroscopy and gravimetric method was built. Then the laser confocal micro Raman spectrometer was used to visualize the *S. obliquus* at 0–10 day, and the correlation model between the total lipid content measured by Raman spectroscopy and gravimetric method was also built. Then the THz model was compared with the Raman model.

## Results

### Content and composition of lipids in *Scenedesmus obliquus*

As shown in Fig. 1a, the variation rule of lipids was found out it increases first and then decreases, and reaches the highest value on the eighth day. The total lipid content of *S. obliquus* was 18.1% on day 0. On the eighth day, the lipid content reached 50.8%, which was 2.8 times of the initial value. We also used GC-MS to analyze the proportion of fatty acids in lipids and the variation in the fatty acid profile of *S. obliquus* in stress culture are summarized (Tab. 1). The proportion of SFA has reduced by 45% and the proportion of UFA has increased by 12% from day 0 to 8. GC-MS combined with dry weight method showed that the dry weight ratio of UFA increased from 11.16% to 44.51%, while the dry weight ratio of SFA decreased from 6.90% to 6.28% on the 0-8 day.

### Microscopic examination of *Scenedesmus obliquus*

Image can contain a lot of biological information. Obtain intuitive and clear images in the field of microbiological research, which can better analyze the characteristics and status of specific areas of cells or organisms, as well as the distribution of specific molecules. NR result indicated lipid substances widely exist in cells and cells of *S. obliquus* appear yellow-orange in a fluorescence microscope after lipid staining. With the presence of accumulated oil droplets, they turn bright yellow. The Fig. 1b shows the fluorescence microscopic observation of different lipid accumulation in *S. obliquus* cells. However, due to the limited resolution of fluorescence microscopy, we used high-resolution TEM to supplement the

observation of the microstructure of *S. obliquus*. The observed results were presented in Fig. 2. The study indicated that oil droplets were located near the cell membrane in the cytoplasm, and were mostly light gray circles or ellipses in TEM observation field.

### **Observation of *Scenedesmus obliquus* lipids by Raman spectroscopy**

The effective band of  $900\text{cm}^{-1}$  to  $1700\text{cm}^{-1}$  was processed with the methods of cosmic rays' removal, Savitzky-Golay smoothing and baseline correction [27-29]. As shown in Fig. 3a, the Raman spectroscopy of *S. obliquus* had a few peaks at 965, 1005, 1160, 1187, 1266, 1353, 1445, and  $1525\text{ cm}^{-1}$ , which correspond to the metabolic components in *S. obliquus* [30-35]. Studies have shown that the corresponding H-C=bending plane at  $1266\text{ cm}^{-1}$  mainly represented the fatty chain unsaturation [33], and the corresponding C-H<sub>2</sub> bending bond at  $1445\text{ cm}^{-1}$  mainly represented the saturated carbon chain [12,36]. After analyzing the Raman curve above, we further performed imaging analysis, and tried to compare the results with NR and GC-MS to verify the feasibility of the results and explore the advantages of Raman in the distribution of *S. obliquus* lipid. Interpolation method was used to map the selected characteristic peaks into pseudo-color images of lipid distribution. Generally, the redder the color in the captured image, the more lipids, and vice versa. As shown in Fig. 3b, the pseudo-color map of the distribution of UFA in the cells of *S. obliquus* was plotted with a peak value of  $1266\text{ cm}^{-1}$  and the pseudo-color map of total fatty acids (TFA) distribution was plotted with the  $1445\text{ cm}^{-1}$  peak value after correction.

It can be observed from the distribution of unsaturated fatty acids in *S. obliquus* cells that the UFA are discontinuously distributed, and most of them are distributed in the two regions of the cells. The red area in the cell indicates the accumulation of UFA. The darker the color, the higher the UFA content. Comparing the NR and TEM results with the Raman results, the oil droplets were located near the cell membrane in the cytoplasm. Over time, the red area in *S. obliquus* gradually became larger and darker. It was believed that the UFA content gradually increased, and the UFA content was highest on the eighth day. The changes of pseudo-color maps of TFA and UFA are similar. The above results show that Raman spectroscopy is effective for the detection of intracellular lipid in *S. obliquus*.

### **Metabolic analysis by Terahertz**

#### **Band assignments**

Some previous studies have shown that pure categories such as proteins, lipids, carbohydrates and carotenoids can be identified by THz molecular vibrational spectroscopy techniques. The main components of *S. obliquus* are protein, lipids, carbohydrate and carotenoids and their THz absorption spectra are distributed in the different frequency ranges: 3.3-5.0 THz for proteins [15,37], 2.3, 9.3, 9.4, 9.8, 11.4 THz for lipids [25,26], 9.0, 10.5, 12.1, 13.1 16.0, 17.2 and 18.0 THz for carbohydrates [16,38], 12.1, 14.7, 15.6 and 19.6 THz for  $\beta$ -carotene [39]. THz has been used for the study on different types of lipids and fatty acids [25,26]. For example, saturated fatty acids (SFA) such as palmitic acid and stearic acid

have distinct peaks at 9.3 and 9.4 THz, respectively. Unsaturated fatty acids (UFA) such as oleic acid, linoleic acid and linolenic acid all have two distinct peaks at 7.4 and 9.8 THz. In general, lipids usually show broader and distinct absorption peaks. In the spectra of *S. obliquus* cells, the peak of 9.3 THz corresponded to the C=O and -COO- vibration [26]. This peak mainly represented the lipids. The broad band of 3.3-5 THz corresponded to the population of overlapping discrete vibrational modes from the random amino acid sequences. It is similar to other globular proteins, such as myoglobin, hemoglobin, and lysozyme, which showed that microalgae proteins lack of highly repetitive segments in their amino acid sequences [15,37]. The peaks of 15.6-18.0 THz mainly corresponded to the C-C-O, C-O-C, C-C-C covalent skeletal deformation [16,38,39]. These peaks are fused due to changes in the corresponding substance content, resulting in a significant absorption peak in the spectra of *S. obliquus*.

### **Relating changes in Terahertz band under nitrogen stress**

After confirming the corresponding absorption peak of main components in microalgae, analysis of several main absorption peaks in the *S. obliquus* spectra can reflect the changes of the main components, such as proteins, carbohydrate, lipids, carotenoids in the *S. obliquus*. Changes in the THz band and its corresponding components during microalgal metabolism were analyzed under nitrogen stress. During the nitrogen stress culture, the protein content of the microalgae cells continues to decrease, the lipid content increased first and then decreased with its maximum on the eighth day. The carbohydrates first increased and then stabilized, the  $\beta$ -carotene content of the *S. obliquus* cells continued to increase. As shown in Fig. 4a, the absorption band of 3.3-5 THz was red-shifted, which may be due to the changes in protein types of the cells. A study of microalgae showed that nitrogen starvation triggers the accumulation of multiple proteins associated with oxidative phosphorylation [4], such as NADH dehydrogenase, ATP synthase and cytochrome oxidase. In general, this absorption band strength is gradually reduced because of the increase in nitrogen stress time. Absorption peaks of  $\beta$ -carotene and carbohydrates are difficult to distinguish at the band 15-18 THz. But from the red and blue shift of the absorption peak, the carbohydrate and  $\beta$ -carotene response and cumulative speed can be found. The carbohydrates rapidly accumulate, resulting in a blue shift, such as the fourth day. The  $\beta$ -carotene accumulates rapidly, resulting in a red shift, such as the tenth day. Nitrogen deficiency induces  $\beta$ -carotene accumulation, but the response speed is significantly behind that of carbohydrates.

### **PCA and PLS modeling based on THz spectroscopy**

Spectra in the range of 2-20 THz for each day were further analyzed by PCA algorithm to distinguish these ingredients. THz spectra of the cells in different culture days showed obvious clustering in PC-1 and PC-2 directions (Fig. 4b). PC1 and PC2 explained together 96% of the variation in the spectra (83% by PC1 and 13% by PC2). The aggregation of algae samples is mainly affected by protein, carbohydrate, lipid and pigment content. Among them, the decrease of protein content and the increase of lipid content have the greatest influence. Combining the results shown in Fig. 2a and Fig. 2b, the absorbance value of lipids changes most obviously at 0-10 days, which is consistent with the clustering effect of samples analyzed by PCA at 0-10 days. PCA analysis shows that the THz spectra of *S. obliquus* can be effectively

distinguished for different grown days under nitrogen stress, and it is feasible to analyze the changes of microalgae metabolites.

THz data were divided into modeling set and predicting set with a ratio of 2:1. Using PLS algorithm to model the data of modeling set to discriminate different days (0, 2, 4, 6, 8, 10 day) of nitrogen stress. When building PLS prediction model, the accuracy of prediction model is determined by comparing correlation coefficient and root mean square error of calibration set and prediction set. It can be seen from Tab.2 that the correlation coefficient of prediction model at each stress time point is above 0.991, and the RMSE is less than 0.020. These results indicated that the model constructed by THz spectrum of full band can discriminate *S. obliquus* cells under different nitrogen stress culture times effectively, and accuracy of the model was relatively high. On this basis, we combined THz bands to model and obtained better results, which means that this prediction method was effective.

### **Quantitative analysis of lipid by Terahertz and Raman spectroscopy**

As shown in Fig. 5a, we have established a correlation model between the absorbance value at the 9.3 THz and the reference lipid content by gravimetric method, the model had determination coefficient ( $R^2$ ) of 0.96. The Raman model established based on the Raman intensity of the lipid characteristic peak ( $1445\text{cm}^{-1}$ ) has an  $R^2$  of 0.85 (Fig. 5b). The accuracy of Raman model coefficient is lower than the THz of this research. The above results show that THz spectroscopy is effective for the detection of intracellular lipids in *S. obliquus*. THz signal can be a useful spectroscopy for monitoring microbial metabolism.

## **Discussion**

The gravimetric method relies on solvent-based lipid extraction, which is usually time-consuming, insensitive to small differences in lipid content, and requires large amounts of cellular material and toxic solvents. In addition, since traditional gravimetric methods involve multiple steps, some neutral lipids may be lost. NR can directly observe lipid accumulation, but there are some limitations, such as spectral interference with chlorophyll autofluorescence, non-specific fluorescence and inconsistent cell absorption. TEM can clearly analyze the structure of cells and organs from a micro perspective, but the cost is too high, which is suitable as a supplementary method. GC-MS can get the specific composition of lipids, but the sample pretreatment method is destructive, time consuming, and not environmentally friendly and does not allow for real-time lipid content monitoring. Both THz spectroscopy and the confocal Raman spectroscopy are fast, non-invasive method for the lipids monitoring in microalgae. When monitoring lipid changes in *S. obliquus*, Raman can visualize lipids in microalgae, but its quantitative models are generally less accurate than THz. THz provides a new spectral analysis method for detecting microalgae lipids, which can provide technical supporting for the engineering culture of oil-producing microalgae under environmental control in future.

## **Conclusions**

This paper proposes to use THz spectroscopy to study the changes in the composition of lipids, proteins, carbohydrates,  $\beta$ -carotene and through these changes to distinguish *S. obliquus* cells of different days and lipid content. Principal component analysis (PCA) and partial least squares (PLS) are used to distinguish and predict microalgae from different stress days. The correlation coefficient of the model prediction results is greater than 0.991, and the root mean square error is less than 0.020. It indicated that THz technology can be used to monitor the change of material composition in microalgae under nitrogen stress. A correlation model between THz and gravimetric analysis was established, with a model accuracy of up to 0.96. The THz lipid quantitative model was used to compare with the Raman lipid quantitative model. For the observation of lipids using spectroscopic techniques, the THz is significantly more accurate than Raman. For the study of microalgae metabolites, THz technology is in its infancy, and there is still much room for research.

## Material And Methods

### Culture conditions

*S. obliquus*, FACHB-12, was purchased in Freshwater Algae Culture Collection at the Institute of Hydrobiology, FACHB-collection. *S. obliquus* was cultivated in an ultra-clean platform, in which the temperature was set at about 25°C, the light intensity was 2500 Lux, and the light and illumination dark period was 12 h:12 h. The normal BG11 basal medium was configured according to the standards provided by the Institute of Hydrobiology.

*S. obliquus* was expanded in BG11 medium for about 2 months and cultured to a stable growth stage, and microalgae were harvested for experiments. The algal fluid was centrifuged by a centrifuge, and the supernatant was decanted so as to reserve the bottom algal puree. And then the algal puree was washed twice with ultrapure water. Finally, the algal puree which has removed solute was harvested. 1.5 g/L NaNO<sub>3</sub> in normal BG11 medium was reduced to 0.5 g/L to prepare the nitrogen-deficient medium. The harvested algal puree was cultivated in media with the 2000 ml of the algal fluid volume. The algal fluid was placed in the ultra-clean platform and the cultivation conditions were consistent with the original cultivation conditions. Before each experiment, the microalgae cell concentration was estimated by the cell count plate method to ensure that the microalgae were in stable growth throughout the experimental period.

### Gravimetric method

(1) Algae powder weighing: the clean centrifugal tube was weighed ( $W_0$ ) and the clean Petri dish was dried to constant weight ( $W_1$ ). 50 ml of algae solution was centrifuged at the speed of 9000 r/min for 15 minutes. The liquid supernatant was removed and then the tube was dried in a 50°C oven to constant weight ( $W_2$ ).

(2) Chlorophyll destruction: the dried algal flour adding a 3ml mixture of 5% KOH and 30% methanol was placed in a 50°C water bath for 15 minutes. After that it was still standing for 4 hours and then

centrifuged at 7000 r/min for 5 minutes.

(3) Crude lipid extraction: 2 ml water, 4 ml methanol, and 4 ml chloroform were added into the centrifuged tube and shaken for 5 minutes.

(4) Weigh: Transfer all chloroform layer to the clean Petri dish in step (1), place the dish in a fume hood at 25°C to completely volatilize the chloroform, and weigh the dish again ( $W_3$ ).

(5) Lipid content calculation:

### **Determination of lipid composition**

(1) Algal slurry harvest: 500ml of the uniform algae of *S. obliquus* was taken after collecting the spectrum, and was placed in centrifuge tubes separately centrifuging at a speed of 9000 r/min for 15 minutes. The temperature of the centrifuge was set to 4°C simultaneously. After centrifugation, the supernatant was discarded, and then ultrapure water was added to the remaining algal slurry to vibrate into a uniform algae solution. The algae were then centrifuged at the same parameters, and harvested after repeating the ultrapure cleaning process. All algae harvested in the centrifuge tubes were broken by ultrasonic vibration in a 50 ml round-bottom flask for 15 minutes.

(2) Fatty acid extraction: methanol, chloroform, and hydrochloric acid were mixed in a ratio of 10:1:1 to form a reaction mixture. 10 ml of the reaction mixture was added to the algal mud after ultrasonic wave breaking. Then the round bottom flask containing the reactants was refluxed in a water bath at 90°C for 4 hours. The fatty acid was extracted by adding 3 ml of n-hexane, and the extraction was repeated for 3 times. The extract liquor was later transferred to a 10 ml centrifuge tube and then concentrated to 1 ml by nitrogen blowing method.

(3) Chromatography mass spectrometry conditions: using automatic detection program, temperatures of the injection port and detector were set to 250°C and 300°C respectively, the split ratio was 50:1, and the temperature of the oven was controlled in following profile. It was gradually rose from 60°C to 150°C in a speed of 30°C per minute, then it would gradually increase to 240°C at the rate of 13°C per minute and last for 30 minutes, and eventually the oven would heat up to 265°C for 5 minutes.

(4) Result analysis: the collected data were analyzed using the peak area method. And the components were determined by comparing the peaks with NIST mass spectrometry database.

### **Nile Red staining method**

After the *S. obliquus* cell walls were broken, 0.5 ml of DMSO solution was added to 4 ml of the algae solution and mixed for 10 minutes. Then 40µl of NR mother liquor (0.1 g/l) was added and stained for 30 minutes. Finally, the sample was observed in the dark under the fluorescence microscope.

### **Raman spectroscopy collection and processing**

In order to ensure the position of the microalgae cells unchanged when collecting data, the cells are fixed with agar. During the procedure, 3g agar powder was dissolved in 100ml of ultrapure water and then before cooling to 45°C the agar liquid was boiling completely for 3 minutes. After mixing 3 ml agar solution with 1 ml algae solution evenly, the sections were placed on the glass slides for analyzing confocal Raman micro spectroscopy. Firstly, microalgae cells were found by using the microscope section of the Renishaw laser confocal micro Raman spectrometer (Renishaw PLC, United Kingdom/InVia–Reflex 532/XYZ) and were selected by the wire software for acquiring the mapping plots. The prepared sample was fixed on the objective table, the laser beam would emit with a 532 nm argon ion (Ar+) laser (power: 20mW) and focus through a 50X objective onto the surface of the sample 16. Following were the detail setting during the procedures where the exposure time was set to 1s, the laser light intensity was 1%, the scanning range was 600 to 1800 (Raman Shift/  $\text{cm}^{-1}$ ), the scanning step length was 0.7  $\mu\text{m}$ , and the cumulative number of times was one. The entire experiment was conducted at a constant temperature (about 25°C).

Using baseline correction, Savitzky-Golay smoothing and data normalization to pre-process Raman data. Different spectral data processing uses different data normalization formulas. When calculating the Raman intensity, we sum the intensity of the marker bands in all pixels and divide by the number of pixels.

### **Terahertz spectroscopy collection and processing**

The cell suspension was harvested by centrifugation for 5 min at 9000 r/min at ambient temperature, and about 200 mg of algal mud was obtained. The pellets were washed twice with distilled water and the centrifugation was repeated. Then the algae solution concentrated to 1 ml was added to a smooth polyethylene mold with a diameter of 20 mm and dried 6 h at 40°C using a dryer for lipid characterization and biomass composition determination. At this time, the sample was made into a film with a thickness of 20  $\mu\text{m}$ . THz spectra were acquired with a resolution of 0.06THz, and each measurement is an average over 128 sample scans and 128 background scans, in the range between 2 and 20 THz using a Bruker 66v/s Fourier Transform spectrometer. In order to eliminate the absorption contribution from atmospheric water vapour, the entire light path of instrument was a Nidec rotary vacuum pump. The experiment was performed every two days; 8 samples were measured every day, and each sample was measured 5 times repeatedly.

We use Baseline correction and Savitzky-Golay smoothing to pre-process THz data. Then use Principal component analysis (PCA) and Partial least squares (PLS) to classify and predict the data. PCA is an unsupervised learning method and a commonly used data processing method in multivariate statistical analysis. This method can more easily grasp the main contradictions and reduce the complexity of the data by reducing the number of dimensions [10]. The variance of the principal component is greater, and the model reflects more information. The purpose of this method is to simplify the mathematical model and improve the efficiency of data analysis. PLS is a supervised learning method and a multiple linear regression method based on input and predicted values. Use the correlation coefficient of the predicted

value to find the best solution between the data and the model. Multiple regression analysis improves the accuracy of model prediction [11]. The correlation coefficient ( $r$ ) and root mean square error (RMSE) are used to judge the reliability of the model.

## Abbreviations

Scenedesmus obliquus: *S. obliquus*; GC-MS: gas chromatography-mass spectrometry; NR: Nile Red; THz: terahertz; IR: infrared; TEM: transmission electron microscopy; TFA: total fatty acids; SFA: saturated fatty acids; UFA: unsaturated fatty acids; PCA; Principal component analysis; PLS: Partial least squares; RMSE: root mean square error

## Declarations

### Ethics approval and consent to participate

Not applicable.

### Availability of data and material

Not applicable.

### Consent for publication

Submitted for publication.

### Competing interests

The authors declare that they have no competing interests.

### Funding

The research presented in this article was supported by the National Major Project of Scientific Instrument and Equipment Development (2017YFF0106300), Natural Fund Project of Shanghai (18ZR1425700), National Natural Science Foundation of China (61922059, 61771314, 81961138014), Shanghai Rising-Star Program (17QA1402500).

### Authors' contributions

The work presented here was carried out in collaboration between all authors. YS conceived the idea. WG, SW, YQ co-worked on associated data collection and carried out the experimental work. WG drafted the manuscript, YP helped to renew the original paper. YZ and SZ have supported the instrument and technology. All authors read and approved the final version of the manuscript.

### Acknowledgements

Not applicable.

## References

1. Hill J, Nelson E, Tilman D, Polasky S, Tiffany D. Environmental, economic, and energetic costs and benefits of biodiesel and ethanol biofuels. *Proc Natl Acad Sci USA*. 2006;103(30):11206–11210.
2. Katiyar R , Gurjar BR , Bharti RK , Kumar A, Biswas S, Pruthi V. Heterotrophic cultivation of microalgae in photobioreactor using low cost crude glycerol for enhanced biodiesel production. *Renew Energ*. 2017;113:1359-1365.
3. Chisti Y. Biodiesel from microalgae beats bioethanol. *Trends Biotechnol*. 2008;26(3):126-131.
4. Luis Valledor, Takeshi Furuhashi, Luis Recuenco-Muñoz, Stefanie Wienkoop, Wolfram Weckwerth. System-level network analysis of nitrogen starvation and recovery in *Chlamydomonas reinhardtii* reveals potential new targets for increased lipid accumulation. *Biotechnol Biofuels*. 2014;7(1):171.
5. Sun XM, Ren LJ, Zhao QY, Ji XJ, Huang H. Microalgae for the production of lipid and carotenoids: a review with focus on stress regulation and adaptation. *Biotechnol Biofuels*. 2018, 11(1).
6. Griffiths MJ, Harrison STL. Lipid productivity as a key characteristic for choosing algal species for biodiesel production. *J Appl Phycol*. 2009;21:493-507.
7. Chen W, Zhang C, Song L, Sommerfeld M, Hu Q. A high throughput Nile red method for quantitative measurement of neutral lipids in microalgae. *J Microbiol Methods*. 2009;77:41-7.
8. Feng GD, Zhang F, Cheng LH, et al. Evaluation of FT-IR and Nile Red methods for microalgal lipid characterization and biomass composition determination. *Bioresour Technol*. 2013;128(1):107-12.
9. Satpati GG, Mallick SK, Pal R. An alternative high-throughput staining method for detection of neutral lipids in green microalgae for biodiesel applications. *Biotechnol Bioprocess Eng*. 2015;20(6):1044-55.
10. Ge H, Jiang Y, Xu Z, et al. Identification of wheat quality using THz spectrum. *Opt Express*. 2014; 22(10):12533-12544.
11. Ma Y, Wang Q, Li L. PLS model investigation of thiabendazole based on THz spectrum. *J Quant Spectrosc Ra*. 2013; 117(3):7-14.
12. Chiu LD, Ho SH, Shimada R, Ren NQ, Ozawa TI. Rapid in vivo lipid/carbohydrate quantification of single microalgal cell by Raman spectral imaging to reveal salinity-induced starch-to-lipid shift. *Biotechnol Biofuels*. 2017;10(1):9.
13. Samek O, Jonas A, Pilat Z, Zemanek P, et al. Raman microspectroscopy of individual algal cells: Sensing unsaturation of storage lipids in vivo. *Sensors*. 2010;10:8635- 8651.
14. Wang CL, Gong JX, Xing QR, Li YF, Liu F, et al. Application of Terahertz Time-Domain Spectroscopy in Intracellular Metabolite Detection. *J Biophotonics*. 2010;3(10-11):641-645.
15. Han Y, Ling S, Qi Z, Shao Z, Chen X. Application of Far-Infrared Spectroscopy to the Structural Identification of Protein Materials. *Phys Chem Chem Phys*. 2018;10:1039.

16. Nakajima S, Shiraga K, Suzuki T. Quantification of starch content in germinating mung bean seedlings by terahertz spectroscopy. *Food Chem.* 2019;294:203-208.
17. Fischer BM, Walther M, Jepsen PU. Far-infrared vibrational modes of DNA components studied by terahertz time-domain spectroscopy. *Phys Med Biol.* 2002;47(21): 3807-3814.
18. Nagai N, Kumazawa R, Fukasawa R. Direct evidence of inter-molecular vibrations by THz spectroscopy. *Chem Phys Lett.* 2005;413(4–6):495-500.
19. Qin J, Ying Y, Xie L. The detection of agricultural products and food using terahertz spectroscopy: a review. *Appl Spectrosc Rev.* 2013;48(6):439-457.
20. Globus T, Moyer AM, Gelmont B, Khromova T, Lvovska MI, Sizov I, et al. Highly resolved sub-terahertz vibrational spectroscopy of biological macromolecules and cells. *IEEE Sens J.* 2013;13(1):72-79.
21. Zhang W, Brown ER, Viveros L, et al. Narrow terahertz attenuation signatures in *Bacillus thuringiensis*. *J Biophotonics.* 2014; 7(10):818-824.
22. Tyo KE, Hal S. Alper, Gregory N, Stephanopoulos. Expanding the metabolic engineering toolbox: more options to engineer cells. *Trends Biotechnol.* 2007;25(3):132-137.
23. Park SJ, Hong JT, Choi SJ, et al. Detection of microorganisms using terahertz metamaterials. *Sci Rep.* 2014; 4.
24. Globus T, Dorofeeva T, Sizov I, et al. Sub-THz Vibrational Spectroscopy of Bacterial Cells and Molecular Components. *Am J Biomed Eng.* 2012, 2(4):143-154.
25. Jiang FL, Ikeda I, Ogawa Y, Endo Y. Terahertz absorption spectra of fatty acids and their analogues. *J Oleo Sci.* 2011;60(7):339.
26. Jiang FL, Ikeda I, Ogawa Y, et al. Rapid Determination of Saponification Value and Polymer Content of Vegetable and Fish Oils by Terahertz Spectroscopy. *J Oleo Sci.* 2012; 61(10):531-535.
27. Wang T, Ji Y, Wang Y, et al. Quantitative dynamics of triacylglycerol accumulation in microalgae populations at single-cell resolution revealed by Raman microspectroscopy. *Biofuels.*, 2014; 7(1):58.
28. Shao Y, Fang H, Zhou H, et al. Detection and imaging of lipids of *Scenedesmus obliquus* based on confocal Raman microspectroscopy. *Biotechnol. Biofuels.* 2017, 10(1):300.
29. Li Y, Han D, Sommerfeld M, Hu Q. Photosynthetic carbon partitioning and lipid production in the oleaginous microalga *pseudochlorococcum* sp. (chlorophyceae) under nitrogen-limited conditions. *Bioresour Technol.* 2011;102(1):123-129.
30. Wood BR, Heraud P, Stojkovic S, Morrison D, Beardall J, McNaughton D. A Portable Raman Acoustic Levitation Spectroscopic System for the Identification and Environmental Monitoring of Algal Cells. *Anal Chem.* 2005;77(15):4955–
31. Wang X, Sun MJ, et al. Analysis of Astaxanthin in *Phaffia Rhodozyma* Using Laser Tweezers Raman Spectroscopy. *Spectrosc Spect Anal.* 2012;32(9):2433-2437.
32. Chan JW. Recent advances in laser tweezers Raman spectroscopy (LTRS) for label-free analysis of single cells. *J Biophotonics.* 2012;6(1):36–

33. Hosokawa M, Ando M, Mukai S, Osada K, Yoshino T, Hamaguchi H, Tanaka T. In Vivo Live Cell Imaging for the Quantitative Monitoring of Lipids by Using Raman Micro-spectroscopy. *Anal Chem.* 2014;86(16):8224–
34. Sharma SK, Nelson DR, Abdrabu R, Khraiwesh B, Jijakli K, Arnoux, M, et al. An integrative Raman microscopy-based workflow for rapid in situ analysis of microalgal lipid bodies. *Biotechnol Biofuels.* 2015; 8(1):164.
35. Samek O, Zemánek P, Jonáš A, Telle HH. Characterization of oil-producing microalgae using Raman spectroscopy. *Laser Phys Lett.* 2011, 8(10):701-709.
36. Wu H, Volponi JV, Oliver AE, Parikh AN, Simmons BA, Singh S. In vivo lipidomics using single-cell Raman spectroscopy. *Proc Natl Acad Sci USA.* 2011;108:3809-14.
37. Stehle CU, Abuillan W, Gompf B, Dressel M. Far-infrared spectroscopy on free-standing protein films under defined temperature and hydration control. *J Chem Phys.* 2012; 136:075102.
38. Flores-Morales A, M. Jiménez-Estrada, R. Mora-Escobedo. Determination of the structural changes by FT-IR, Raman, and CP/MAS <sup>13</sup>C NMR spectroscopy on retrograded starch of maize tortillas. *Carbohydr Polym.* 2012;87(1):61-68.
39. Zuo J, Zhang L, Yu F, Zhang Z, Zhang C. The observation of terahertz spectra of all-trans beta-carotene molecule. *Proc SPIE.* 2010;7854.

## Tables

**Table 1. Fatty acid composition of *S. obliquus*.**

Fatty acid	Fatty acid content (%)		
	Day 0	Day 4	Day 8
C14:0	8.22	3.24	1.77
C16:0	30.12	19.41	12.35
C16:3	1.80	2.58	2.67
C16:4	10.76	17.55	29.8
C18:1	9.25	12.14	6.41
C18:2	11.37	10.73	7.64
C18:3	24.50	27.10	29.77
C18:4	3.65	6.33	8.55
C20:5	0.33	0.92	1.34
SFA	38.34	22.65	12.38
UFA	61.66	77.35	87.62

Table 2 Prediction of different time under nitrogen stress based on PLS models

Discrimination model	Calibration		Prediction	
	Rc	RMSEC	Rp	RMSEP
o day	0.985	0.020	0.998	0.013
2 day	0.971	0.038	0.991	0.020
4 day	0.998	0.010	0.999	0.006
6 day	0.981	0.017	0.999	0.008
8 day	0.973	0.035	0.999	0.016
10 day	0.973	0.037	0.991	0.018

## Figures

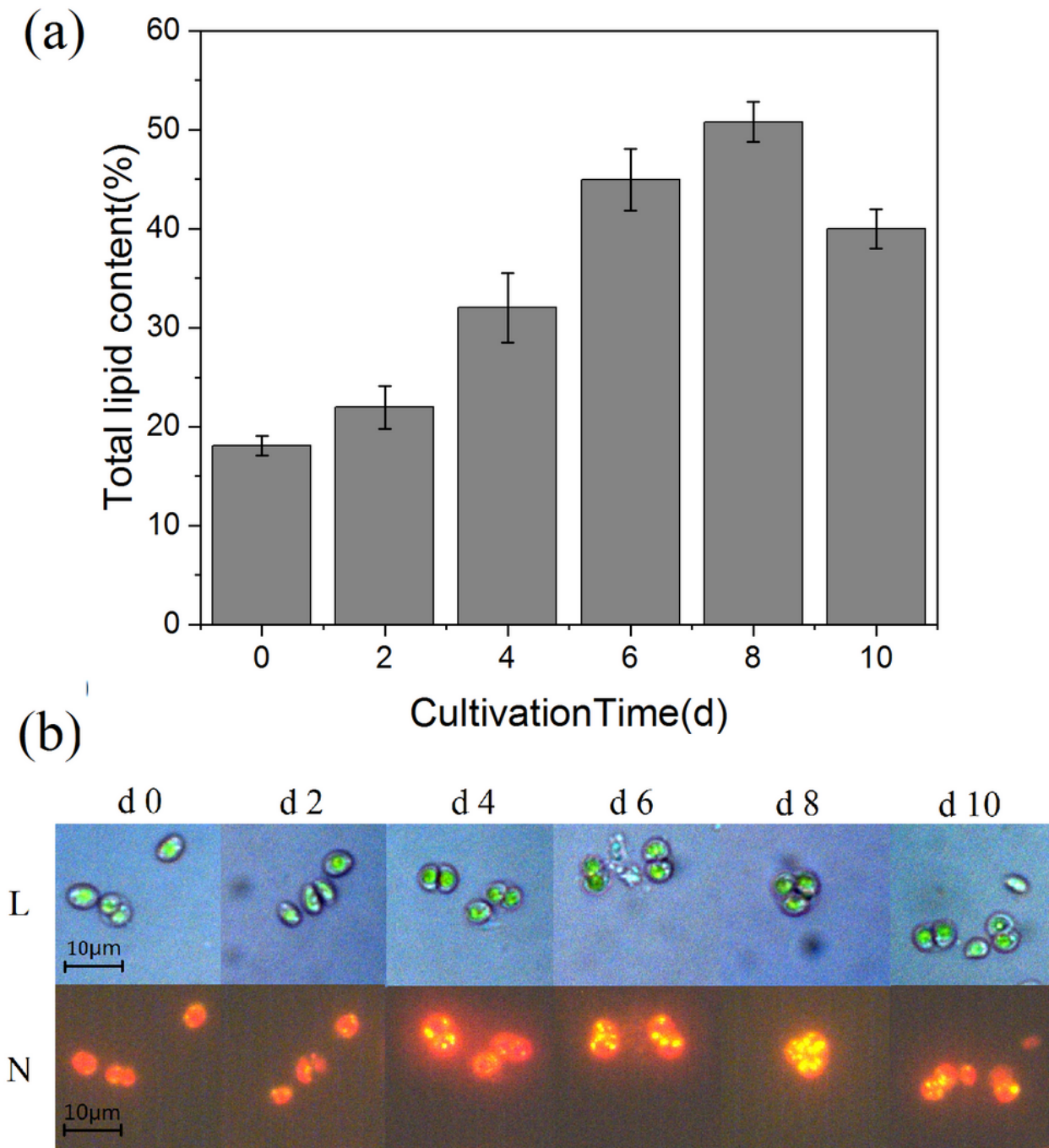


**Figure 1**

(a) Gravimetric methods for lipid content determination and (b) NR fluorescent images of *S.obliquus* at different days.

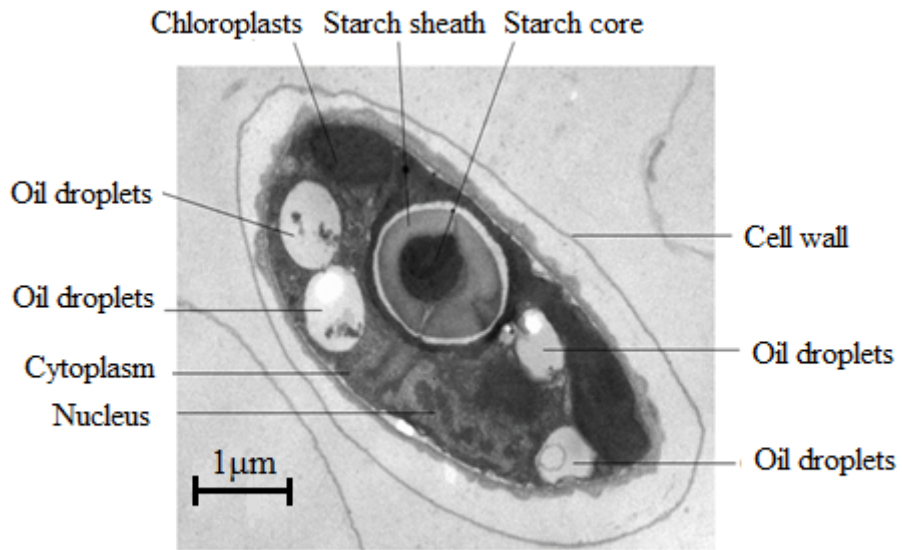


**Figure 2**

Transmission Electron Microscopic observation of *S. obliquus*.

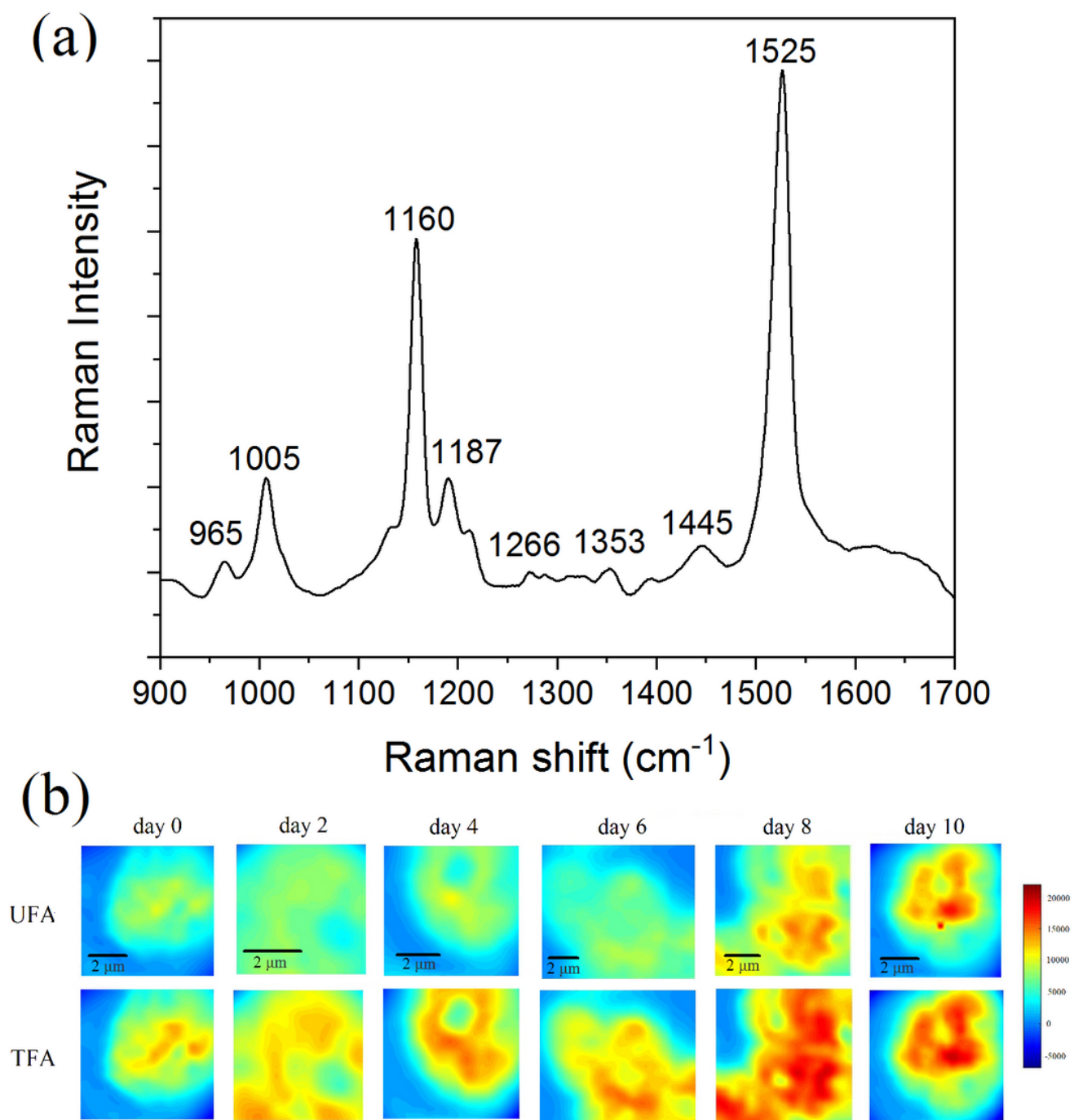


**Figure 3**

(a) Raman spectrum after baseline correction. (b) The pseudo-color maps of fatty acids distribution. (Note: Distribution of UFA was obtained by Raman intensity at 1266cm<sup>-1</sup> and distribution of TFA was obtained by Raman intensity at 1445cm<sup>-1</sup>.)

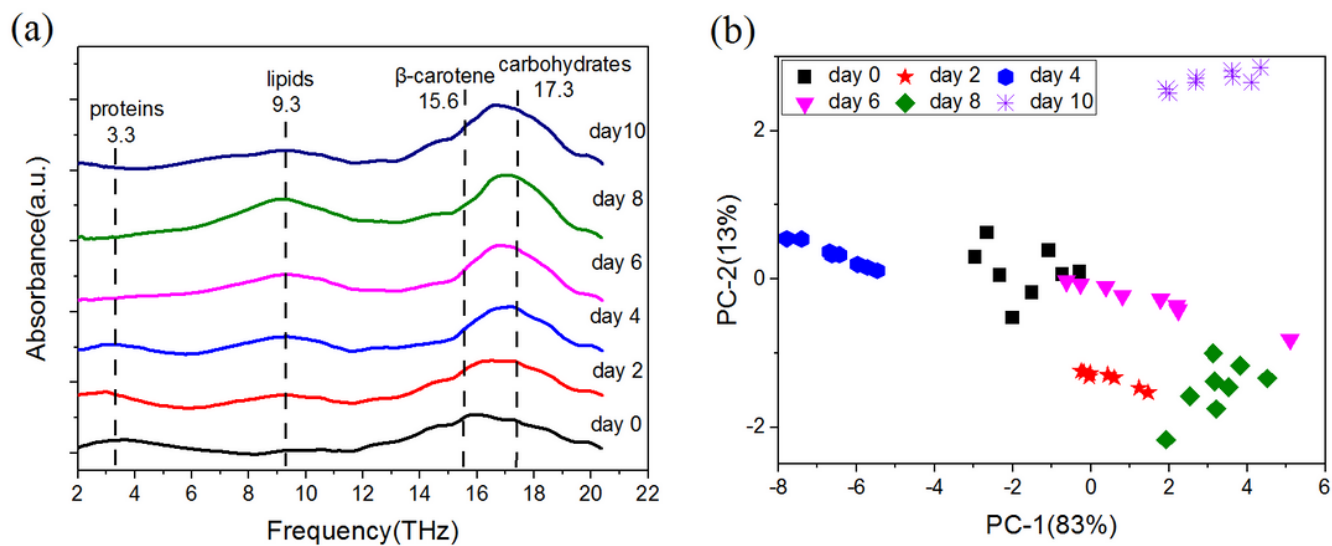


**Figure 4**

(a) Terahertz spectrum after baseline correction. (b) Score plot of PC-1 and PC-2.

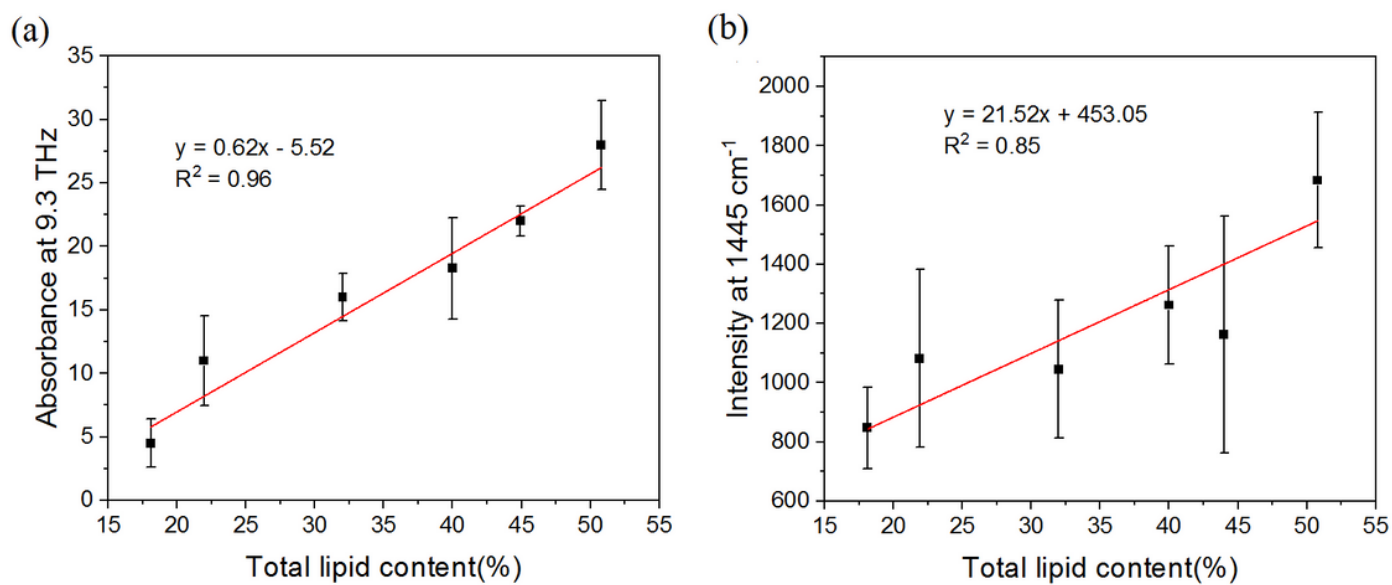


**Figure 5**

Relationships between total lipid contents and (a) terahertz measurement, (b) Raman measurement.